A Numerical Study of the Retrieval of Sea Surface Height Profiles from Low Grazing Angle Radar Data

Joel T. Johnson, Robert J. Burkholder, Jakov V. Toporkov, David R. Lyzenga, and William J. Plant

***Abstract*— A numerical study of the retrieval of sea surface height profiles from low grazing angle radar observations is described. The study is based on a numerical method for electromagnetic scattering from one-dimensionally rough sea profiles, combined with the "improved linear representation" of Creamer et al for simulating weakly non-linear sea surface hydrodynamics. Numerical computations are performed for frequencies from 2975 to 3025 MHz so that simulated radar pulse returns are achieved. The geometry utilized models a radar with antenna height 14 m observing the sea surface at ranges from 520 m to 1720 m range. The low grazing angles of this configuration produce significant shadowing of the sea surface, and standard analytical theories of sea scattering are not directly applicable.**

Three approaches for retrieving sea height profile information are compared. The first method uses a statistical relationship between the surface height and the computed radar cross sections versus range (an incoherent measurement). A second method uses the phase difference between scattering measurements in two vertically separated antennas ("vertical interferometry") in the retrieval. The final technique retrieves height profiles from variations in the apparent Doppler frequency (coherent measurements) versus range, and requires that time-stepped simulations be performed. The relative advantages and disadvantages of each of the three approaches are examined and discussed.

***Index Terms*— Rough surfaces, ocean remote sensing, sea surfaces**

I. Introduction

RADAR systems are commonly used in oceanographic remote sensing to retrieve information on mean sea level (altimetry), significant wave height (altimetry/SAR), wind speed (altimetry/scatterometry/SAR), and wave spectra (SAR as well as other radar types) [1]-[5]. In the past, the primary interest in these quantities has been in their average behaviors, e.g. the sea wind speed averaged over a large spatial scale or the sea wave spectrum averaged over time and space. Recently, retrievals of the deterministic sea height profile have been proposed using tower or ship based radar systems [6]-[9] with both coherent [6] and incoherent [7]-[9] radar systems. Validation of the sea height profiles so retrieved is difficult because obtaining independent measurements of the sea surface height profile is challenging experimentally. However point comparisons of retrieved height information with buoy sea height measurements as a function of time have shown reasonable correlations between the buoy heights and those retrieved from radar measurements [7].

This paper provides further investigation of the potential for radar systems to retrieve sea height profile information through the use of numerical simulations of microwave scattering from ocean-like surfaces. The advantage of such an approach is that deterministic knowledge of the true sea height profile is available for assessing retrieval performance. Three algorithms for retrieving height information are compared.

The simulations performed combine numerical methods for electromagnetics (as in [10]-[14]) with the weakly non-linear hydrodynamic model of Creamer et al [15] so that non-linear hydrodynamic interactions can be included approximately. The current methodology is an extension of similar previous studies [16]-[25] that have gradually increased the complexity and applicability of such combined simulations. The general trend has been from single-frequency scattering from time-evolving surfaces so that Doppler information can be extracted [16]-[22] (note the final reference is one of the few papers performing such studies for surface rough in two dimensions) to multi-frequency scattering simulations with stationary surfaces [23]-[24] so that range-resolved scattering can be investigated, through simulations that include both range resolution (fast time scale) and time evolution (slow time scale) [25] so that range resolved Doppler spectra are achieved. The current paper primarily performs range resolved scattering studies of stationary surfaces, but will also consider range resolved Doppler spectra. Due to the computational complexity of such simulations, the surface profiles considered are rough in one spatial dimension only. The impact of this limitation will be discussed in more detail later in the paper. All simulations considered model a radar with an antenna height 14 m observing the sea surface at ranges 520 m to 1720 m, resulting in local grazing angles ranging from 1.54 to 0.46 degrees.

The next section describes the numerical simulations performed, and attempts to retrieve surface height information from radar cross section information, interferometric information, and from Doppler information are described in subsequent sections. Final conclusions are presented in Section VI.

II. Description of numerical simulations

In general, the simulation procedure used is very similar to that described in [24], and the reader is referred to [24] for additional information. The method of moments with the "novel

Manuscript received Month dd, yyyy; revised Month dd, yyyy. J. T. Johnson and R. J. Burkholder are with The Ohio State University, Dept. of Electrical and Computer Engineering and ElectroScience Laboratory. Jakov V. Toporkov is with the Naval Research Laboratory. David R. Lyzenga is with the Dept. of Naval Architecture and Marine Engineering, The University of Michigan. Willian J. Plant is with the Applied Physics Laboratory of the University of Washington.

spectral acceleration" method [12]-[14] is used to compute backscattered fields from a set of ocean-like surface profiles. Sea surfaces are modeled using an impedance boundary condition with a relative dielectric constant of $73 + i35$. Surface profiles are 1200 m in length, and scattering is computed at 512 frequencies from 2975 to 3026.1 MHz. This bandwidth when weighted by a Hanning window produces a 3.4 m 3-dB range resolution when transformed to the time domain. The profile length used represents roughly 12000 electromagnetic wavelengths, and the surface is discretized into 131072 points in the computations.

The illuminating field is essentially that of a point source located 14 m above the mean surface height and 520 m from the left surface edge; an "r-card" treatment [26] of width 46 m at surface edges is used to reduce surface edge scattering effects. Scattered power information from points within 50 m of surface edges will be discarded in what follows. Received fields are computed at the transmitter antenna location, as well as locations displaced vertically upward with respect to the transmit antenna in order to allow interferometric studies.

The surface profiles simulated are Gaussian stochastic processes with a Pierson-Moskowitz spectrum (parametrized solely by wind speed), passed through the transformation of Creamer et al [15] to obtain weakly non-linear surfaces. This transformation approximates both non-linear long wave effects (i.e. slightly sharper crests and flatter troughs) as well as long-short wave interactions, as will be shown in what follows. A wind speed of 15 m/s was used to produce the set of surfaces with rms height 1.17 m and significant wave height 4.67 m.

Simulations were performed using parallel computing resources at the Maui High Performance Computing Center, and required approximately 1 minute per frequency. A complete simulation of 512 frequencies for 2 incident polarizations required approximately 18 hours, with 64 realizations achieved by using 64 processors.

Following the computation of received fields versus frequency, an evaluation of time domain fields is performed using a Fourier transform process. In particular, the received field corresponding to a particular spatial location (i.e. a particular time) is obtained by summing frequency domain fields with the phase delay of the two-way path to the particular location compensated, assuming the point of interest is at the mean sea surface height. This phase delay is modified appropriately for shifted vertical locations of the received field. Received fields versus range were computed on an oversampled grid of 8192 spatial points (0.147 m sampling distance), but averaging over space was later used as will be explained subsequently. Appropriate scale factors are included so that the final received powers as a function of spatial position correspond to normalized radar cross section (NRCS) quantities, as defined in [27] for one-dimensionally rough surfaces.

Two specific simulation types were performed: in the first, range resolved fields were computed for a set of 64 stationary surface realizations. The entire dataset of field returns can then be compared with the corresponding surface height and/or slope information in order to develop retrieval procedures. In the second type, a single surface realization was evolved in time over 128 timesteps of 5 msec each, so that range-resolved Doppler information could be computed and compared to surface heights and/or slopes.

III. Incoherent (NRCS) retrievals

For radar observations at larger grazing angles than those considered here, it is well known that range resolved RCS measurements provide information on wave features that are large compared to the radar spatial resolution. Under the composite surface model of sea surface scattering, measured NRCS values vary along long waves due to a "tilt" mechanism (i.e. a change in the radar local incidence angle due to long wave slopes) and a hydrodynamic mechanism in which amplitudes of the short waves responsible for Bragg scattering vary with position along the long wave [28]-[31]. For the Creamer et al surfaces considered here, average hydrodynamic modulations are essentially in phase with surface height variations (as in [32]-[33]) while tilt modulations are in phase with the surface slope.

Reference [7] describes an approach for estimating sea surface slope information given measurements of the NRCS versus range by considering tilt modulations only. In this approach, the mean over time of NRCS values versus range is subtracted, and the remaining modulations are converted into local surface slopes by examining variations of composite surface model predictions with incidence angle. Retrieved slopes are then integrated over space to obtain surface height, and also passed through a space-time filtering process centered on the gravity wave dispersion relation in order to reduce retrieval errors.

While such an approach may be applicable for larger grazing angles, it is clear that shadowing effects not considered in the composite surface model can be appreciable for low grazing incidence geometries. Reference [8] attempts to address shadowing issues through a numerical ray-tracing approach, and suggests that NRCS modulations are more likely to be related to surface height, rather than slope, due to the impact of shadowing. Furthermore, a recent study using combined numerical scattering and hydrodynamic surfaces [23] at larger grazing angles showed the composite surface model approach to achieve only moderate accuracy in matching observed NRCS variations.

Given these uncertainties and the strong impact of shadowing for ship-based radar systems, a statistical approach is adopted here to interpret the relationship between NRCS values and surface heights or slopes. Previous numerical simulations of low grazing angle backscattering from one dimensional impedance surfaces [11], [12] offer some insight into this process. At very low grazing angles and for one dimensionally rough surfaces of small roughness, the NRCS is essentially proportional to the grazing angle raised to a specific power, equal to the third power in the limit of very small surface roughness [9]. However, for rougher surfaces and at grazing angles that are not negligibly small, the NRCS versus grazing angle appears proportional to an exponential function of the grazing angle, so that the NRCS in decibels has a linear dependence on the grazing angle. The latter is more consistent with predictions of the composite surface theory [11].

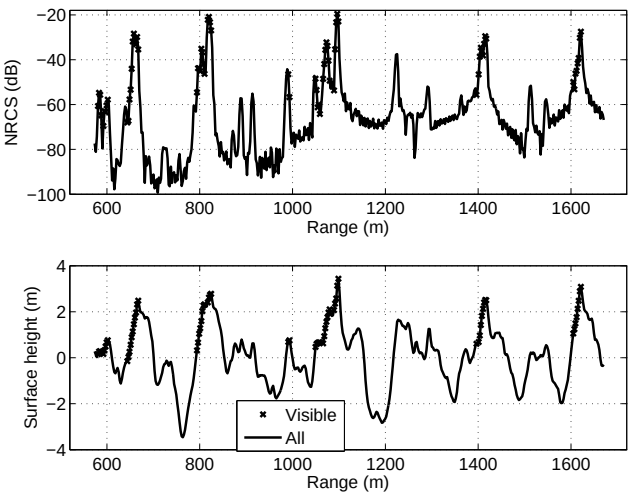

Fig. 1. Sample HH range resolved NRCS (dB) (upper) for one of the sixty four surface realizations considered (lower).

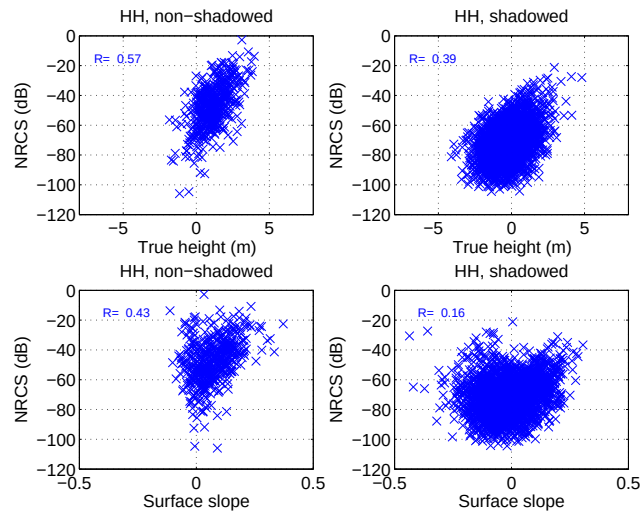

Fig. 2. Scatter plots of HH NRCS values for non-shadowed (i.e. visible, left) and shadowed (right) portions of surfaces versus surface height (upper) or slope (lower). Correlation coefficients between NRCS and height or slope indicated in corresponding plots.

The dataset of NRCS values versus 8192 points in range was first averaged to 512 points (a spatial sampling distance of 2.34 m), and points near surface edges were discarded to obtain 469 NRCS values in 64 surface profiles, a total of 30016 points. The corresponding surface heights and slopes were computed for these NRCS values by passing the true surface profile (resolved at 9.2 mm spatial resolution) though a Gaussian low pass filter to obtain a spatial resolution of approximately 2 m. Figure 1 illustrates the range resolved HH NRCS for one of the surface realizations considered (surface profile illustrated in the lower plot of Figure 1.) The range resolved NRCS plot shows very strong contrasts of up to 70 dB over the surface, essentially describing a scattering process dominated by a few localized scatterers rather than an area extensive surface. A comparison with the corresponding surface profile shows the dominant scatterers to be located along points of larger surface heights, where shadowing is less likely to occur. A simple algorithm based on tracing rays from the transmitter location to a given location on the surface was used to classify points as visible or shadowed (ray does not or does intersect the surface prior to the point of interest, respectively.) Points classified as visible are marked with symbols in Figure 1, and clearly demonstrate the strong impact of non-local shadowing for this geometry. However, points classified as visible are not uniformly of large NRCS, nor are shadowed points uniformly of small NRCS. Range resolved NRCS returns in VV polarization are very similar to those in HH polarization but are 15 to 20 dB larger; no "sea-spike" behaviors are observed in the results obtained, likely due to the absence of any breaking wave behaviors in the Creamer et al hydrodynamic model.

The large contrasts observed between the typical NRCS of shadowed and visible regions in Figure 1 makes clear that both extremely high dynamic ranges and signal-to-noise ratios would be required for realistic radar systems to measure returns both in the visible and shadowed regions. In practice, it is unlikely that sufficient signal-to-noise ratios would be achieved in order to provide observations of the NRCS in shadowed regions. The following results assume an infinite signal-to-noise ratio; retrievals performed in the presence of additive receiver noise would likely show much poorer performance in the shadowed portions of the surface than those illustrated.

Statistical tests were performed by correlating the range-resolved NRCS (linear units) raised to an arbitrary power with the corresponding surface slopes (equal to variations in the local grazing angle.) Such tests showed poor correlations in general between NRCS and surface slopes for a wide range of considered exponents. Greatly improved correlations were observed between surface properties and the NRCS in decibels, so this approach was utilized in the retrieval process. In this process, no strong variations in the correlations or in the mean NRCS values were observed versus range (a 0.46 to 1.54 degree grazing angle range) although the number of points utilized is insufficient to resolve any smaller variations.

Figure 2 provides a scatter plot of HH NRCS values, separated into shadowed and visible portions of the surface as classified by the ray tracing algorithm, versus both the corresponding surface heights and slopes. Figure 2 generally shows an approximate linear dependence of the NRCS in decibels versus both surface height and slope, particularly for the visible portions of the surface. Correlations are larger to surface height than to slopes, even following the separation into shadowed and visible regions. A moderate correlation to surface height exists even for the shadowed portions of the surface. Similar results (not shown) are obtained in VV polarization, with an even larger ($R = 0.5$) correlation in the shadowed region to surface heights.

Given the partial correlation observed both to surface height and slope, the influence of phase shifting the surface profile on observed correlations was also examined. Figure 3 in the upper plot illustrates the correlation observed between the visible surface HH NRCS in dB and the phase shifted surface height, as a function of the phase shift utilized. The phase shifting operation is achieved by Fourier transforming the

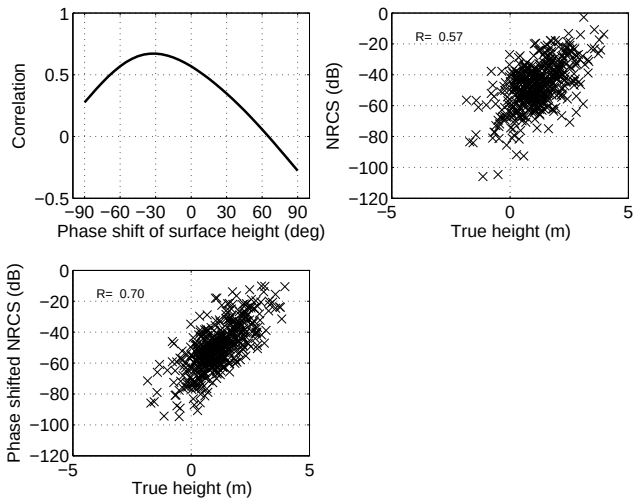

Fig. 3. Investigation of the impact of phase shifting the NRCS in dB on correlation to surface height. Upper left: correlation of NRCS in dB with surface height as a function of the phase shift of surface height. Upper right: Original scatter plot of visible HH NRCS with surface height. Lower left: Scatter plots of visible HH NRCS with surface height following phase shifting operation.

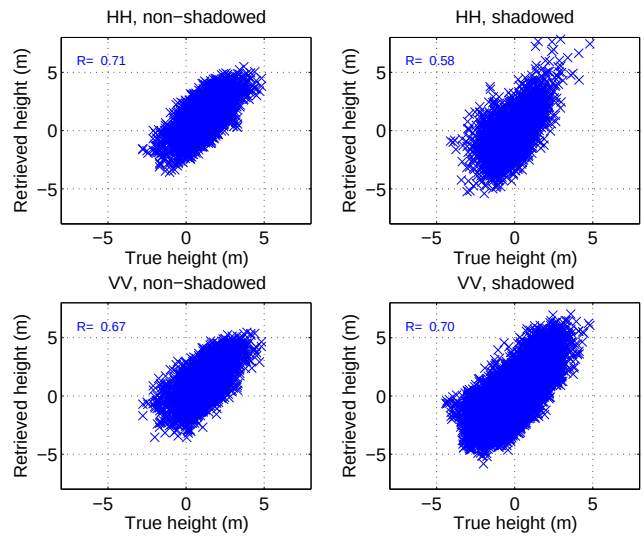

Fig. 4. Scatter plots of true and retrieved surface profiles, with correlations of true and received profile heights indicated in the figures.

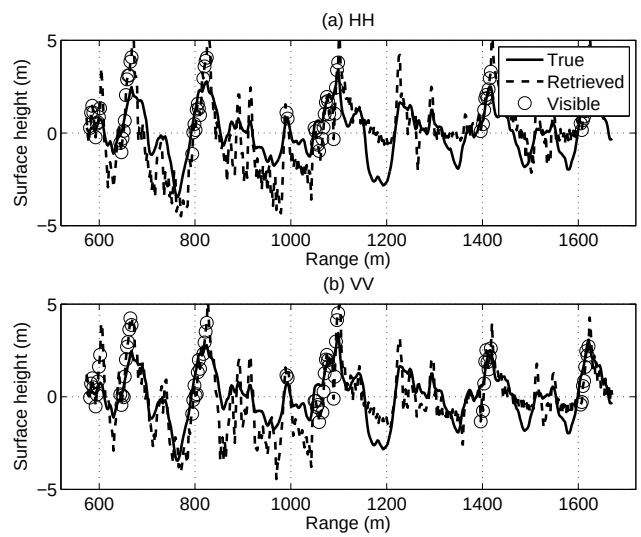

Fig. 5. Sample NRCS-based surface profile retrievals for HH (upper) and VV (lower) polarizations.

surface profile, adjusting the phase of the surface Fourier coefficients by the specified phase shift, and then transforming back to the space domain. The results show that the maximum correlation is achieved when the surface height is phase shifted by -30 degrees, so that the obtained quantity is "in-between" the surface height and slope phase behaviors. The upper right plot of Figure 3 illustrates the original scatter plot of the NRCS versus surface height, while the lower left plot illustrates the corresponding scatter plot when the NRCS in phase shifted by $+30$ degrees. The result shows an improved correlation of 0.7 compared to 0.57 for the original NRCS. Similar results are obtained for VV polarization and for the non-shadowed cases, although the phase shifts utilized are distinct, and also when correlations to surface slopes are examined.

At this point, a quasi-linear relationship between phase-shifted NRCS values in dB and either surface height or slope has been observed. Given a statistically determined linear fit to the NRCS versus either surface height or slope, it is then possible to retrieve height or slope estimates from measured NRCS data. Retrieval of slope information requires an additional step of integration if the surface height profile is of interest; such an integration can cause long wave (i.e. low spatial frequency) errors in the surface profile. For simplicity, here a direct retrieval of surface height was instead utilized. Retrievals of surface slopes using a similar procedure (not shown) produced similar results, and the apparent "tilt" modulation coefficient was found to be significantly larger than that predicted by the composite surface model.

Figure 4 provides a scatter plot of true and retrieved surface heights following this procedure, with distinct fits performed in the visible and shadowed regions and for HH and VV polarizations. The results show reasonable retrievals for visible portions of the surface, and also indicate that NRCS measurements contain information in the shadowed surface portions. Retrieval accuracies are similar for HH and VV, although HH retrievals are more degraded in the shadow regions than VV. Standard deviations of errors are 0.98 and 1.07 m in HH and VV visible points, respectively, and 1.52 and 1.12 m in shadowed regions, respectively.

Figure 5 plots an example retrieved profile using both HH and VV polarizations. Comparison of the true and retrieved profiles shows the NRCS retrieval to capture many of the basic surface height features, but also to contain significant errors of 1.37 and 1.06 m standard deviation in HH and VV polarizations for this particular surface. The clear degradation of the retrieval in shadowed regions is apparent; again a realistic radar system operating with a reasonable signal-to-noise ratio would show further degradation in retrievals in the shadowed portions of the surface.

Overall, these results demonstrate the capability of NRCS measurements for retrieving sea surface profile information.

However the process utilized (a linear relationship between the phase-shifted NRCS in dB and the surface height) was statistically determined, and not well predicted by standard theories of sea surface scattering. In practice, knowledge of these relationships would have to be obtained empirically, and would require extensive field measurements.

It is also noted that the one-dimensional surface geometries considered here are not completely descriptive of all the retrieval issues that could be encountered for a two-dimensional surface. In particular, radar look geometries that are perpendicular to any dominant sea wave directions could show retrieval behaviors that are distinct from those modeled here. In the limit of a true "tilt" modulation process, it would be expected that profile retrieval is very difficult for a cross-wave look geometry, since strong variations in the local angle of incidence do not occur along the range direction in such cases. Further studies with two-dimensional surface models, beyond the scope of the current work, are required to investigate such differences.

IV. Interferometric Retrievals

A surface height profile retrieval method that does not require empirically determined information can be developed using interferometry [6]. Such retrievals are based on the phase difference between observed fields from two antennas displaced vertically. Simulations were performed to include vertical antenna separations of 1, 5, and 10 m; here only the 5 m separation is used, but results are similar for the other antenna height separations. Given the fact that the transformation of received fields versus frequency to the range resolved NRCS already takes into account the difference in path length to the individual antennas (assuming a flat surface profile), the remaining phase difference, Φ, is directly proportional to surface height h through

$$\Phi = kh\left(\sin\theta_2 - \sin\theta_1\right) \approx kh\frac{B}{R} \tag{1}$$

where k is the electromagnetic wavenumber and θ_2 and θ_1 are the grazing angles from a point on the mean surface to the two antennas. The final approximation, which holds for the low grazing angles of interest here, includes the ratio of the "baseline" distance (B, i.e. the vertical separation between the antennas) to the total range R from the center of the antennas to the mean surface point of interest. The final equation makes clear that only moderate phase shifts are observed in the simulations performed, so that no phase wrapping is encountered.

Beginning with the NRCS versus range as described previously, the "interferogram" (i.e. the product of the received field versus range with the conjugate of that from the second antenna) is originally resolved into 8192 spatial points. This quantity is then averaged over 21 points (a spatial sampling distance of ~ 3.1 m) before the phase of the interferogram, Φ, is computed. The above equation is then utilized to estimate surface height from the interferogram phase. Note additional averaging over spatial scales is often used in interferometry to reduce retrieval errors, but was not considered here.

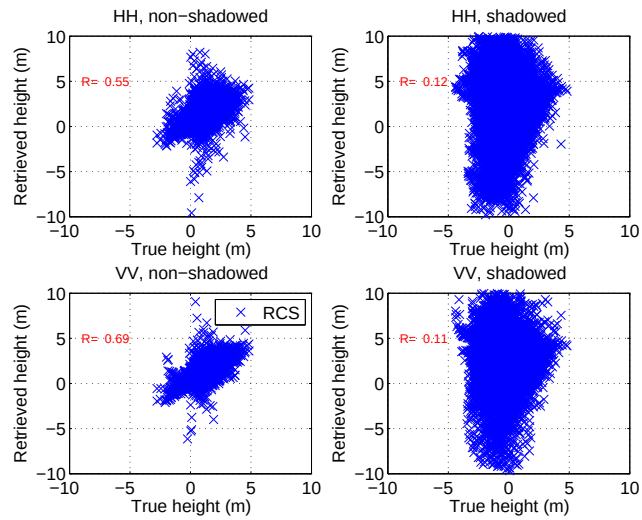

Fig. 6. Scatter plots of true and retrieved surface profiles from interferometric retrievals, with correlations of true and received profile heights indicated in the figures.

Figure 6 provides a scatter plot comparing true and retrieved surface heights following this process, again separated into visible and shadowed portions of the surface and into HH and VV polarizations (all retrievals performed in an identical manner.) A performance that is similar to, but slightly degraded from, that of the NRCS retrievals is observed for the visible portions of the surface, with VV polarization showing improved performance compared to HH polarization. Retrieval accuracy is much worse in the shadowed portions of the surface when compared to that achieved for the NRCS, indicating that the simple point scatter model used to relate surface height to interferogram phase is not applicable for shadowed portions of the surface profile. Error standard deviations are 0.9 and 0.6 m for HH and VV polarizations, respectively, in the visible portions of the surface, but degrade to 2.5 and 2.3 m in the shadowed portions. The sample retrieved profile in Figure 7 further highlights the lack of information obtained in shadowed portions of the surface, as well as the greatly improved performance observed in visible portions of the surface. Note that separation of measurements into likely shadowed and likely visible portions can be accomplished with reasonable accuracy based on received power levels.

While interferometric retrievals clearly are not useful for shadowed portions of the surface, their use in visible regions is desirable due to the fact that no empirical knowledge is required. In addition, it is expected that interferometric retrievals should retain the ability to retrieve surface heights even in a cross-wave look geometry for two dimensional surfaces.

V. Doppler Retrievals

The final retrieval process considered is based on use of the range-resolved Doppler spectrum. Under the small perturbation theory of sea scattering, sea surface Doppler responses occur only at frequencies corresponding to the along-range velocity of the Bragg waves of the surface. The two-scale

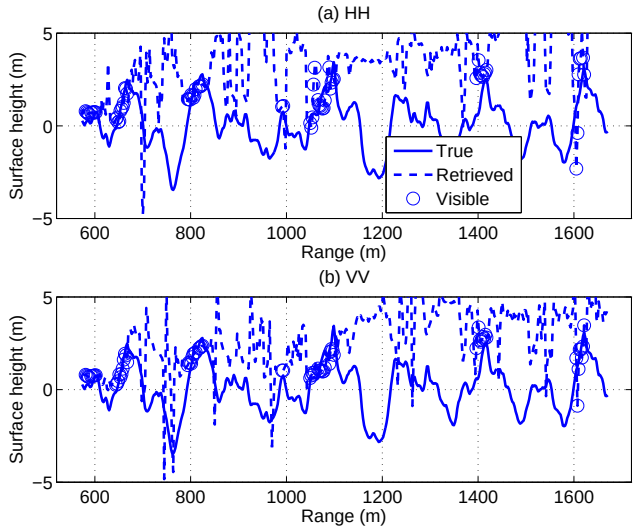

Fig. 7. Sample retrieved profile using interferometric retrieval for HH (upper) and VV (lower) polarizations.

theory for linear hydrodynamic surfaces shows such responses to be broadened in frequency due to the tilting process, and further broadening occurs due to any finite time duration used in estimating the Doppler spectrum. The first moment of the obtained Doppler spectrum (i.e. the Doppler "centroid" frequency) nevertheless remains near that expected for Bragg scatterers in the sea surface.

Measurements at low grazing angles however have shown Doppler spectra to be centered on frequencies shifted with respect to the Bragg wave velocity, typically at locations corresponding to velocities larger than those of the Bragg wave ("fast" scatterers.) Numerical simulations of low grazing angle Doppler spectra have also shown such shifts when non-linear surface profiles are included.

For Doppler spectra resolved in range, it is also known that modulations of the Doppler centroid versus range occur due to the impact of any range-resolved long wave features. Such modulations have been shown to correspond to the orbital velocity of the long waves, so that local shifts in the apparent velocity of sea scatterers are equal to the local orbital velocity. While this modulation is a non-linear hydrodynamic interaction between long and short sea waves (range resolved Doppler simulations using linear hydrodynamic models show no significant variations in the observed Doppler centroid frequency versus range), long wave orbital velocity profiles retrieved through this process can be transformed under a linear model to obtain an estimate of surface height.

The retrieval process thus consists of converting the observed Doppler centroid frequencies into velocities, followed by an inversion of this orbital velocity versus range into the surface height under linear hydrodynamic theory. The latter step involves Fourier transforming the estimated orbital velocity versus range, dividing each Fourier component by the gravity wave angular frequency ω of each sea surface wave, then inverse transforming to obtain the estimated sea surface height. Note the Doppler centroid frequency averaged over range is not important in this process, as it contributes only to constant offset in the surface profile that can be removed by assuming that the surface profile has zero mean over range.

Simulations of range-resolved Doppler spectra were performed by time stepping a single surface realization through 128 time steps of 5 msec each. This 0.64 second duration yields a resolution of 1.56 Hz in the Doppler domain for Doppler frequencies up to ± 100 Hz. Only a single surface realization was considered due to the requirement for computations at multiple time steps.

Simulated normalized Doppler spectra in decibels for VV polarization are illustrated in Figure 8 as a gray-scale image. Two normalizations are illustrated: the first (upper plot) normalizes the image by a single maximum that is taken over all frequencies and ranges, so that relative power variations between visible and shadowed regions remain. The second normalization (lower plot) scales the Doppler spectrum at each range location by its maximum over frequency, so that Doppler spectra remain observable both in the visible and shadowed portions of the surface. Variations in the Doppler spectrum with range due to long wave influences are clearly observable, showing that the Creamer et al model captures the relevant long-short sea wave interactions of this phenomenon. Although the ability to obtain Doppler information in deep shadowed portions of the surface is clearly degraded (surface profile illustrated in Figure 9), useful information is still achieved. Similar results are obtained for Doppler spectra in HH polarization. Again the introduction of receiver noise into this process would degrade the ability to infer Doppler information in the shadowed portions of the surface. Mean Doppler centroids over range are 10.5 and 12.3 Hz in HH and VV polarizations, respectively, corresponding to along range velocities of 52.5 and 61.3 cm/s. The Bragg wave phase velocity here is 27.9 cm/s (Doppler frequency 5.6 Hz) so that these results show "fast" scattering behaviors.

Figure 9 plots the Doppler centroid frequency versus range in VV polarization in the upper plot, and the resulting surface profile retrieval in the lower plot. Although standard deviations of the error are 1.07 m, comparable to those for the NRCS retrievals, Figure 9 suggests that Doppler retrievals yield an improved match to surface profile information in general compared to both the NRCS and interferometric methods. The retrieval performance shows that orbital velocity information is observable even in shadowed portions of the surface, although again signal-to-noise ratios must be sufficient to allow surface scattering to be measured in such regions. Performance in HH polarization is similar but with an error of 0.91 m.

Figure 10 compares surface profile retrievals for the time evolving surface from Doppler (upper), interferometric (middle), and NRCS (lower) algorithms. Interferometric and NRCS retrieved profiles are averaged over the 128 time steps used in the Doppler simulation, and interferometric retrievals are not plotted for shadowed surface points. The results show that all three algorithms can provide information on surface height, with the Doppler retrieval showing good performance throughout the profile, the NRCS retrieval showing more small scale retrieval error, and interferometric retrieval showing reasonable success only in visible portions of the surface.

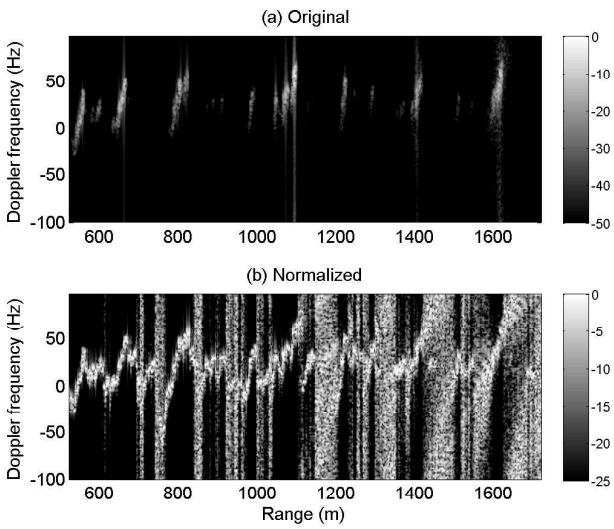

Fig. 8. Normalized Doppler spectra versus range in VV polarization. Color scale in decibels. Corresponding surface profile is illustrated in Figures 9 and 10. Upper plot normalizes the image by the maximum over all ranges and frequencies, while the lower plot normalizes the Doppler spectrum at each range by its maximum over frequency.

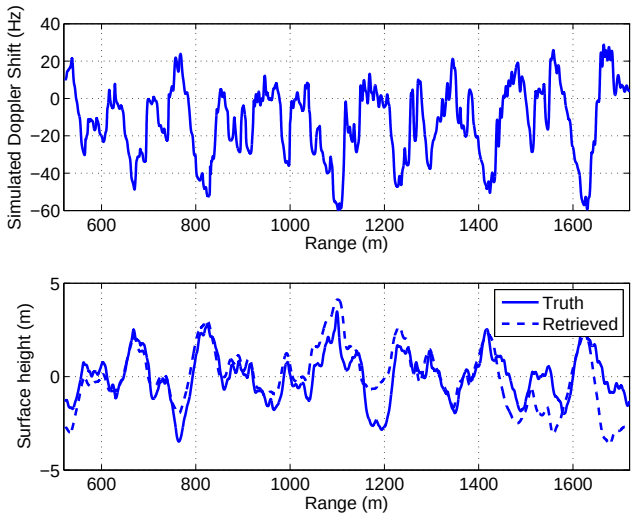

Fig. 9. Doppler centroid frequency versus range for VV polarization (upper) and Doppler surface profile retrieval (lower).

VI. Conclusions

The studies of this paper have shown basic approaches for retrieving sea surface profile information from low grazing angle radar measurements. Due to the failure of the composite surface model for the low grazing angle geometries considered here, a statistical approach was applied to determine an approximate linear relationship between the phase shifted observed NRCS in decibels and the surface height. This relationship appears plausible due to the importance of shadowing effects, although a similar retrieval could also be utilized between a phase shifted surface slope quantity and the NRCS in decibels. Unfortunately, it is not possible a-priori to predict properties of the linear fit and phase shift without empirical data, making NRCS retrievals subject to fit errors in practice. Interferometric data did not require any empirical

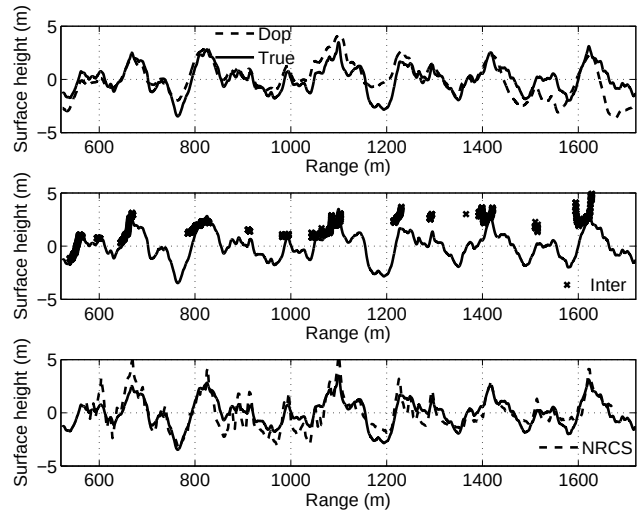

Fig. 10. Comparison of surface profile retrievals for time evolving surface simulation. Doppler (upper plot), interferometric (middle), and NRCS (lower) algorithms are shown.

parameters in the retrieval process, but was found to have information on surface heights only in the visible portions of the surface. Doppler retrievals also required no empirical parameters, and were found to yield reasonable performance both in visible and shadowed portions of the surface.

The results of this study, though informative, are not completely descriptive of practical sea surface applications for several reasons. First, no consideration of true signal-to-noise ratios was included; the high dynamic range exhibited by the NRCS versus range clearly will make signal-to-noise ratios important in practice. Reduced signal-to-noise ratios would quickly eliminate information in any of these techniques for the shadowed portions of the surface. Second, practical systems would likely record observations over an extended period of time, enabling the possibility of averaging retrieved profiles over time and including a space-time filtering operation similar to that described in [7] for reducing retrieval errors. Simulations of such filters are currently in progress and will be reported in future work. Finally, the use of a one-dimensional sea surface model ensures that all tilts and sea surface velocities are in the radar look direction; tilts and velocities in the cross-look direction would likely be much more difficult to observe with NRCS and Doppler systems, although not necessarily with interferometric systems.

These facts make clear that a role will likely exist for all three of these techniques in future sea profile observing instruments. Interferometric methods would be very useful in cross-wave geometries (visible surface portions only), while Doppler and NRCS information would potentially extend information into shadow regions for along-look geometries. Improvements in the basic retrieval algorithms presented here are also likely to be achievable if a complete statistical analysis is performed to determined more optimal methods, including approaches that combine NRCS, interferometric, and Doppler information simultaneously, as well as improved methods for assessing performance beyond the simple rms errors and correlations considered here. Continued studies and experiments in these

areas are planned for the future.

VII. Acknowledgments

The support of the Office of Naval Research MURI on "Optimum vessel performance in non-linearly evolving wave fields," is acknowledged. Use of parallel computing resources at the Maui High Performance Computing Center (MHPCC) is also acknowledged.

References

[1] Ulaby, F. T., R. K. Moore, and A. K. Fung, *Microwave Remote Sensing: Active and Passive,* Norwood, MA: Artech House, 1986.

[2] Jackson, F. C. and D. R. Lyzenga, "Microwave techniques for measuring directional wave spectra," Chapter 14 in *Surface Waves and Fluxes,* vol. 2, Geernaert, G. L. and W. J. Plant, eds., 1990.

[3] Jackson, F. C., W. T. Walton, and P. L. Baker, "Aircraft and satellite measurement of oceanic wave directional spectra using scanning beam microwave radars," *J. Geophys. Res.,* vol. 90, pp. 1005-1018, 1985.

[4] Walsh, E. J., D. W. Hancock, D. E. Hines, R. N. Swift, and J. F. Scott, "Directional wave spectra measured with the surface contour radar," *J. Phys. Ocean.,* vol. 15, pp. 566-592, 1985.

[5] Plant, W. J., W. C. Keller, and K. Hayes, "Simultaneous measurement of ocean winds and waves with an airborne coherent real aperture radar," *J. Atmos. Ocean. Tech.,* vol. 22., pp. 832–846, 2005.

[6] Eshbaugh, J. V. and S. J. Frasier, "Measurement of sea surface displacement with interferometric radar," *J. Atmos. Ocean. Tech.,* vol. 19, pp. 1087–1095, 2002.

[7] Dankert, H. and W. Rosenthal, "Ocean Surface Determination from X-band Radar-Image Sequences," *Journal of Geophysical Research,* vol. 109, C04016, 2004.

[8] Nieto-Borge, J. C., G. R. Rodriguez, K. Hessner, and P. I. Gonzalez, "Inversion of marine radar images for surface wave analysis," *J. Atmos. Ocean. Tech.,* vol. 21, pp. 1291–1300, 2004.

[9] Pan, G., R. J. Burkholder, J. T. Johnson, J. V. Toporkov, and M. A. Sletten, "Studies of ocean surface profile retrieval from simulated LGA radar data," *Intl Geoscience and Remote Sensing Symposium,* conference proceedings, 2006.

[10] J. T. Johnson, R. T. Shin, J. A. Kong, L. Tsang, and K. Pak, "A numerical study of the composite surface model for ocean scattering," *IEEE Trans. Geosc. Remote Sens.,* vol. 36, no. 1, pp. 72-83, 1998.

[11] J. T. Johnson, "A numerical study of low grazing angle backscatter from ocean-like impedance surfaces with the canonical grid method," *IEEE Trans. Ant. Prop.,* vol. 46, no. 1, pp. 114-120, 1998.

[12] Chou, H.-T. and J. T. Johnson, "Novel Acceleration algorithm for Forward-Backward method in the computation of scattering from rough surfaces," *Radio Science,* vol. 33, no. 5, pp. 1277-1287, 1998.

[13] H. T. Chou and J. T. Johnson, "Formulation of forward-backward method using novel spectral acceleration for the modeling of scattering from impedance rough rough surfaces," *IEEE Trans. Geosc. Remote Sens.,* vol. 38, no. 1 (part II), pp. 605–607, 2000.

[14] Torrungrueng, D., J. T. Johnson, and H. T. Chou, "Some issues related to the novel spectral acceleration method for the fast computation of radiation/scattering from one dimensional extremely large scale quasi-planar structures," *Radio Science,* vol. 37, pp. 3(1)-3(20), 2002.

[15] Creamer, D., F. Henyey, R. Schult, and J. Wright, "Improved linear representation of ocean surface waves," *Journal of Fluid Mechanics,* vol. 205, pp. 135161, 1989.

[16] C. L. Rino, T. L. Crystal, A. K. Koide, H. D. Ngo, and H. Guthart, "Numerical simulation of backscatter from linear and nonlinear ocean surface realizations," *Radio Sci.*, vol. 26, no. 1, pp. 51–71, 1991.

[17] Ungan, B. and J. T. Johnson, "Time statistics of propagation over the ocean surface: a numerical study," *IEEE Trans. Geosc. Remote Sens.,* vol. 38, no. 4, pp. 1626–1634, 2000.

[18] J. V. Toporkov and G. S. Brown, "Numerical simulations of scattering from time-varying, randomly rough surfaces," *IEEE Trans. Geosci. Remote Sens.*, vol. 38, no. 4, pp. 1616–1625, 2000.

[19] J. T. Johnson, J. V. Toporkov, and G. S. Brown, "A numerical study of backscattering from time-evolving sea surfaces: comparison of hydrodynamic models," *IEEE Trans. Geosci. Remote Sens.*, vol. 39, no. 11, pp. 2411–2420, 2001.

[20] Toporkov, J. V. and G. S. Brown, "Numerical study of the extended Kirchhoff approach and the lowest order small slope approximation for scattering from ocean-like surfaces: Doppler analysis ," *IEEE Trans. Ant. Prop.*, vol. 50, pp. 417–425, 2002.

[21] A. R. Hayslip, J. T. Johnson, and G. R. Baker, "Further numerical studies of backscattering from time evolving non-linear sea surfaces," *IEEE Trans. Geosci. Remote Sens.*, vol. 41, no. 10, pp. 2287–2293, 2003.

[22] Saillard, M., P. Forget, G. Soriano, M. Joelson, P. Broche, and P. Currier, "Sea surface probing with L-band Doppler radar: experiment and theory," *C. R. Physique,* vol. 6, pp. 675–682, 2005.

[23] Toporkov, J. V. and M. A. Sletten, "Estimation of modulation transfer function from direct numerical simulations of range-resolved backscatter from ocean-like surfaces," *National Radio Science Meeting,* proceedings, 2006.

[24] Toporkov, J. V. and M. A. Sletten, "Statistical Properties of Low-Grazing Range-Resolved Sea Surface Backscatter Generated Through Two-Dimensional Direct Numerical Simulations," *IEEE Trans. Geosc. Rem. Sens.*, vol. 45, pp. 1181-1197, 2007.

[25] Toporkov, J. V. and M. A. Sletten, "Numerical Study of Low Grazing Range-Resolved Radar Backscatter from the Sea Surface," *DoD HPC Users Group Conference*, proceedings, pp. 58–64, Nashville, TN, IEEE Computer Society, June 2005.

[26] West, J. C., "On the control of edge diffraction in numerical rough surface scattering using resistive tapering," *IEEE Trans. Ant. Prop.,* vol. 51, pp. 3180–3183, 2003.

[27] Tsang, L., J. A. Kong and K.-H. Ding, *Scattering of Electromagnetic Waves,* John Wiley & Sons, Inc., New York, 2000.

[28] W. Alpers and K. Hasselmann, "The two-frequency microwave technique for measuring ocean-wave spectra from an airplane or statellite," *Boundary Layer Meteorol.*, vol. 13, pp. 215–230, 1978.

[29] W. J. Plant, "The modulation transfer function: concept and applications," in *Radar Scattering from Modulated Wind Waves* (G. J. Komen and W. A. Oost, eds.), pp. 155–172, Norwell, Mass.: Kluwer Academic, 1989.

[30] T. Hara and W. J. Plant, "Hydrodynamic modulation of short wind-wave spectra by long waves and its measurement using microwave backscatter," *J. Geophys. Res.*, vol. 99, no. C5, pp. 9767–9784, 1994.

[31] R. Romeiser, A. Schmidt, and W. Alpers, "A three-scale composite surface model for the ocean wave-radar modulation transfer function," *J. Geophys. Res.*, vol. 99, no. C5, pp. 9785–9801, 1994.

[32] Pan, G. and J. T. Johnson, "A numerical study of the modulation of short sea waves by longer waves," *IEEE Trans. Geosc. Rem. Sens.*, vol. 44, pp. 2880-2889, 2006.

[33] Pan, G. and J. T. Johnson, "A numerical method for studing modulation effects in radar observations of the sea surface," submitted to *IEEE Trans. Geosc. Rem. Sens.*, 2008.

[34] Rosen, P. A. et al, "Synthetic aperture radar interferometry," *Proc. IEEE,* vol. 88, pp. 333–382, 2000.